Synthetic and Systems Biotechnology 6 (2021) 335–342

Contents lists available at ScienceDirect

Synthetic and Systems Biotechnology

journal homepage: www.keaipublishing.com/en/journals/synthetic-and-systems-biotechnology

Screening and engineering of high-activity promoter elements through transcriptomics and red fluorescent protein visualization in *Rhodobacter sphaeroides*

Tong Shi [a,1], Lu Zhang [a,1], Mindong Liang [a], Weishan Wang [b], Kefeng Wang [a], Yue Jiang [a], Jing Liu [a], Xinwei He [a], Zhiheng Yang [a], Haihong Chen [a], Chuan Li [a], Dongyuan Lv [a], Liming Zhou [a], Biqin Chen [c], Dan Li [c], Li-Xin Zhang [a], Gao-Yi Tan [a,*]

[a] *State Key Laboratory of Bioreactor Engineering (SKLBE), And School of Biotechnology, East China University of Science and Technology (ECUST), Shanghai, 200237, China*

[b] *State Key Laboratory of Microbial Resources and CAS Key Laboratory of Pathogenic Microbiology and Immunology, Institute of Microbiology, Chinese Academy of Sciences (CAS), Beijing, 100101, China*

[c] *Inner Mongolia Kingdomway Pharmaceutical Co., Ltd, Hohhot, 010206, China*

ARTICLE INFO

Keywords:
Rhodobacter sphaeroides
Promoter library
Transcriptomics
Co-enzyme Q_{10}
Red fluorescent protein

ABSTRACT

The versatile photosynthetic α-proteobacterium *Rhodobacter sphaeroides*, has recently been extensively engineered as a novel microbial cell factory (MCF) to produce pharmaceuticals, nutraceuticals, commodity chemicals and even hydrogen. However, there are no well-characterized high-activity promoters to modulate gene transcription during the engineering of *R. sphaeroides*. In this study, several native promoters from *R. sphaeroides* JDW-710 (JDW-710), an industrial strain producing high levels of co-enzyme Q_{10} (Q_{10}) were selected on the basis of transcriptomic analysis. These candidate promoters were then characterized by using *gusA* as a reporter gene. Two native promoters, P_{rsp_7571} and P_{rsp_6124}, showed 620% and 800% higher activity, respectively, than the *tac* promoter, which has previously been used for gene overexpression in *R. sphaeroides*. In addition, a P_{rsp_7571}-derived synthetic promoter library with strengths ranging from 54% to 3200% of that of the *tac* promoter, was created on the basis of visualization of red fluorescent protein (RFP) expression in *R. sphaeroides*. Finally, as a demonstration, the synthetic pathway of Q_{10} was modulated by the selected promoter T334* in JDW-710; the Q_{10} yield in shake-flasks increased 28% and the production reached 226 mg/L. These well-characterized promoters should be highly useful in current synthetic biology platforms for refactoring the biosynthetic pathway in *R. sphaeroides*-derived MCFs.

1. Introduction

With the emergence and development of synthetic biology, the great potential of microorganisms as cell factories that can produce chemicals, pharmaceuticals and nutraceuticals has been extensively studied [1–3]. In addition to traditional microbial cell factories (MCFs) such as *Escherichia coli*, *Saccharomyces cerevisiae* and *Streptomyces* [4,5], several biosynthetically talented strains with special metabolic capabilities, *e.g.,* the thermophilic bacterium *Geobacillus thermoglucosidasius* [6] and the halophilic bacterium *Halanaerobium saccharolyticum* [7], have been engineered to serve as a chassis for biotechnological applications. Recently, the α-proteobacterium *Rhodobacter sphaeroides*, a facultative photosynthetic bacterium [8] with promising potential, has been significantly advanced as a novel MCF for industrial applications [9]. Because of its high metabolic versatility (*e.g.,* photoautotrophic, photoheterotrophic and chemoheterotrophic), a variety of value-added products, such as coenzyme Q_{10} (Q_{10}) [10–13], isoprenoids (*i.e.*, lycopene and β-carotene) [14–17], 5-amino-ketone pentyl acid [18] and even bio-hydrogen [19,20] can be efficiently produced in this cell factory. Therefore, developing a synthetic biology toolbox for *R. sphaeroides*

Peer review under responsibility of KeAi Communications Co., Ltd.

* Corresponding author.
E-mail address: tangy@ecust.edu.cn (G.-Y. Tan).

[1] These authors contributed equally to the paper as first authors.

https://doi.org/10.1016/j.synbio.2021.09.011
Received 5 August 2021; Received in revised form 20 September 2021; Accepted 23 September 2021

would facilitate refactoring of synthetic pathways for bioproduct production and further expand the biotechnology application potential of *R. sphaeroides*.

To date, several toolboxes for *R. sphaeroides*, *e.g.,* a CRISPR/Cas9-based genome editing system [21] and CRISPR/dCas9-based programmable base editing systems [22], have been developed. However, although promoters are among the most important and universal synthetic modular regulatory elements [23–25], only a very limited number of promoters are available in *R. sphaeroides*. Lu et al. first applied the *tac* promoter, a glucose inducible promoter in *E. coli*, for gene overexpression in *R. sphaeroides* [26]. Since then, the *tac* promoter has been widely used in the upregulation of target genes or synthetic modules in *R. sphaeroides* [11,15,17,27–29]. Some other promoters, such as $P_{A1/04/03}$, P_{lac}, P_{puc} and P_{puf}, *etc.*, have also been developed or applied in *R. sphaeroides* for the control of transcription units [15,22,30–32]. Nevertheless, with the increasing number of applications of *R. sphaeroides* in current biotechnology, well-characterized or quantitatively measured high-activity promoters are urgently needed for the precise design or control of synthetic modules in this novel cell factory.

R. sphaeroides JDW-710 (JDW-710) is a high-yielding industrial strain used for Q_{10} production [12], and it is also a nonpathogenic and generally regarded as safe (GRAS) microbial strain [9]. In this study, on the basis of transcriptomic analysis of JDW-710 and the use of a red fluorescent protein (RFP) reporter system, a native promoter-derived synthetic promoter library incorporating a range of different strengths was characterized. To demonstrate the application of these constitutive promoters, we modulated the synthetic pathway of the value-added nutraceutical Q_{10} for overproduction in JDW-710.

2. Materials and methods

2.1. Strains and culture conditions

All strains and plasmids used in this study are shown in Tables S1 and S2. *R. sphaeroides* and its derivatives were cultivated on agar plates (0.3% glucose, 0.8% yeast extract, 0.2% sodium chloride, 0.13% monobasic potassium phosphate, 0.0125% magnesium sulfate and 1.5% agar, supplemented with 15 mg/L biotin, 1 mg/L thiamine hydrochloride and 1 mg/L nicotinic acid) or 20% TSB (trypticase soy broth) medium at 32 °C in 48-well microplates. *E. coli* DH10b was used for plasmid propagation and was cultivated in Luria-Bertani (LB) medium (10 g/L tryptone, 5 g/L yeast extract and 10 g/L sodium chloride, pH 7.0) at 37 °C.

2.2. Plasmid construction, error-prone PCR and transformation

Plasmid pBBR1MCS2 (pBBR) was digested by *Bam*HI and *Sac*I to obtain a linear vector, and a high fidelity GXL polymerase (TaKaRa) was used to amplify the promoter sequence by using *R. sphaeroides* genomic DNA as a template. The gusA gene was chemically synthesized after codon optimization on the basis of a previously reported DNA sequence [23] and also amplified by GXL polymerase. For promoter library construction, error-prone PCR was performed with a Diversify PCR Random Mutagenesis Kit (Clontech). The linear vector DNA and PCR products were assembled with a NovoRec® Plus one step PCR Cloning Kit (Novoprotein, China). All primer sequences used for plasmid construction are shown in Table S3. The electro-transformations of *R. sphaeroides* was performed in 2-mm cuvettes with a Bio-Rad GenePulser Xcell™ system (electroporator conditions: 2000 V, 20 Ω and 25 μF).

2.3. GusA enzymatic assays

R. sphaeroides transformants were cultured in TSB medium or fermentation medium. After sampling at different time points, the amounts of cells were adjusted to OD_{700} = 1.0, and cell pellets were collected by centrifugation (12,000 rpm for 1 min). Subsequently, the cell pellets were resuspended and lysed at 37 °C for 20 min in 900 μL buffer II (50 mM phosphate buffer, pH 7.0, 0.1% Triton X-100, 5 mM dithiothreitol and 1 mg/mL lysozyme). Then, the cell lysate was diluted in 900 μL buffer I (50 mM phosphate buffer, pH 7.0, 0.1% Triton X-100 and 5 mM dithiothreitol), and the supernatant was collected by centrifugation (14,000 rpm, 10 min) at 4 °C. Finally, 100 μL of the resulting supernatant and 100 μL of buffer III (50 mM phosphate buffer, pH 7.0, 0.1% Triton X-100, 5 mM dithiothreitol and 2 mM 4-nitrophenyl-β-D-glucuronic acid) were mixed in 96-well microplates and the absorbance was immediately measured at 415 nm per min for 30 min with a microplate reader (CLARIOstar, BMG LABTECH). The GusA enzymatic activity was determined by calculation according to a previous study [23].

2.4. Red fluorescence analysis

During the promoter library construction, a portable fluorescent protein detector, LUYOR-3260GR and red filter LUV-50-A (Shanghai LUYOR Instrument Co., Ltd), were used to screen *R. sphaeroides* transformants on agar plates. For 48-well microplate culture, the red fluorescence was measured with a BMG CLARIOstar microplate reader (BMG Labtech, UK) with excitation at 570 nm and emission at 620 nm.

2.5. Q_{10} fermentation and cell growth detection

For seed culture, *R. sphaeroides* and its derivatives were cultivated on agar plates for 5 days, and single clones were inoculated in seed medium (1% glucose, 0.1% yeast extract, 0.1% sodium chloride, 0.1% ammonium chloride, 0.01% magnesium sulfate, 0.09% dipotassium phosphate and 0.06% monopotassium phosphate, pH 7.0) and cultured at 32 °C and 220 rpm for 24 h. For the Q_{10} fermentation, 9 mL of seed culture broth was inoculated in a 250-mL flask containing 45 mL of fermentation medium (4% glucose, 0.4% corn steep liquor, 0.3% sodium glutamate, 0.3% ammonium sulfate, 0.28% sodium chloride, 0.3% monobasic potassium phosphate, 0.63% magnesium sulfate and 0.2% calcium carbonate, supplemented with 1 mg/L thiamine hydrochloride, 1 mg/L nicotinic acid and 15 μg/L biotin) and fermented at 220 rpm and 32 °C for 72 h. Growth of *R. sphaeroides* cells was detected by measurement of the optical density at 700 nm (OD_{700}), as previously reported [13].

2.6. Q_{10} detection and high-performance liquid chromatography (HPLC)

Q_{10} production was measured by HPLC, as previously reported [13]. Briefly, 500 μL of fermentation broth was mixed with 5 μL of 6 N hydrochloric acid and 100 μL 30% hydrogen peroxide, 1 mL acetone was added, and the mixture was vortexed for 1 min. Then, the volume was adjusted to 5 mL with ethanol, and incubated in an ultrasonic bath for 45 min at room temperature. The supernatant was collected by centrifugation at 12,000 rpm for 10 min at 4 °C and then passed through a 0.45-μm filter (Merck Millipore). Finally, the resulting samples were used for Q_{10} detection by an Agilent 1260 system (Agilent Technologies, Santa Clara, CA, USA).

2.7. RNA-seq and qRT-PCR assays

RNA-seq was used for transcriptomics analysis, as described previously [33]. Briefly, the quality of the isolated RNA samples was analyzed with an Agilent Bioanalyzer 2100 system (Agilent Technologies), and rRNA depletion was applied for mRNA enrichment. The RNA-seq and transcriptomic analyses were performed by Novogene Co., Ltd. (Beijing, China). The qRT-PCR assays were performed as previously reported [34]. Total RNA was isolated with a Redzol reagent kit from SBS Genetech Co. Ltd (Beijing, China). RNA was purified and reverse transcribed with a commercially available PrimeScript™ RT Reagent Kit with gDNA Eraser (Takara). The qPCR was performed with cDNA as the template

and primers were designed as shown in Table S4. The relative expression levels of *dxs* and *ubiE* were normalized internally to 16 S rDNA level and quantified with the $2^{-\Delta\Delta CT}$ method [35].

2.8. Data analysis

Statistical analyses were performed in Microsoft Excel 2016. Data are expressed as the mean ± standard error of the mean (SEM). Student's *t*-tests were used for statistical analysis, and $P < 0.05$ indicated statistical significance.

3. Results

3.1. Screening and verification of native high-activity promoters

R. sphaeroides carried two different circular chromosomes, namely chromosome I (~3 Mb) and chromosome II (~0.9 Mb) [36]. To screen highly active native promoters from *R. sphaeroides*, we performed transcriptomic analyses of both JDW-710 and the wild type (WT, *R. sphaeroides* 2.4.1) at different time points (24-h and 48-h) by RNA-seq. The transcriptional activity of chromosome I was higher than that of chromosome II (Fig. 1A), and the median transcription levels of chromosome I were 41% and 369% higher than those of chromosome II in JDW-710 and WT, respectively. Therefore, we subsequently analyzed the transcriptional profile of ~3100 genes in chromosome I (Fig. 1B, Fig. S1). On the basis of their FPKM (Fragments Per Kilobase of transcript per Million fragments mapped) values, seven promoters (P_{rsp_2718}, P_{puhA}, P_{pucBAC}, P_{rnpB}, P_{rsp_7571}, P_{bchE} and P_{rsp_6124}) exhibiting high transcriptional activity in both JDW-710 and WT from late logarithmic phase (24 h) to the stationary phase (48 h) were selected as candidates for characterization.

The widely used reporter gene, β-glucuronidase (*gusA*) has been applied in promoter characterization [23]. In this study, the GusA activity of all JDW-710 transformants containing the pBBR plasmid with a different promoter driving *gusA* was analyzed (Fig. 1C). The GusA activity of P_{bchE}, P_{rsp_6124} and P_{rsp_7571} was significantly higher than that of *tac*. Subsequent analysis showed that the activity of P_{rsp_6124} and P_{rsp_7571} was 800% and 620% higher, respectively, than that of *tac* (Fig. 1D). These transcriptional analysis and promoter characterization results indicated that P_{rsp_6124} and P_{rsp_7571} were highly active native promoters in *R. sphaeroides*.

3.2. In vivo characterization of selected promoters

The transcriptional activity of many native promoters is often under strict regulation, and might be affected by changes in external or environmental conditions. Therefore, we characterized the activity of the selected promoters in different culture media at different time periods.

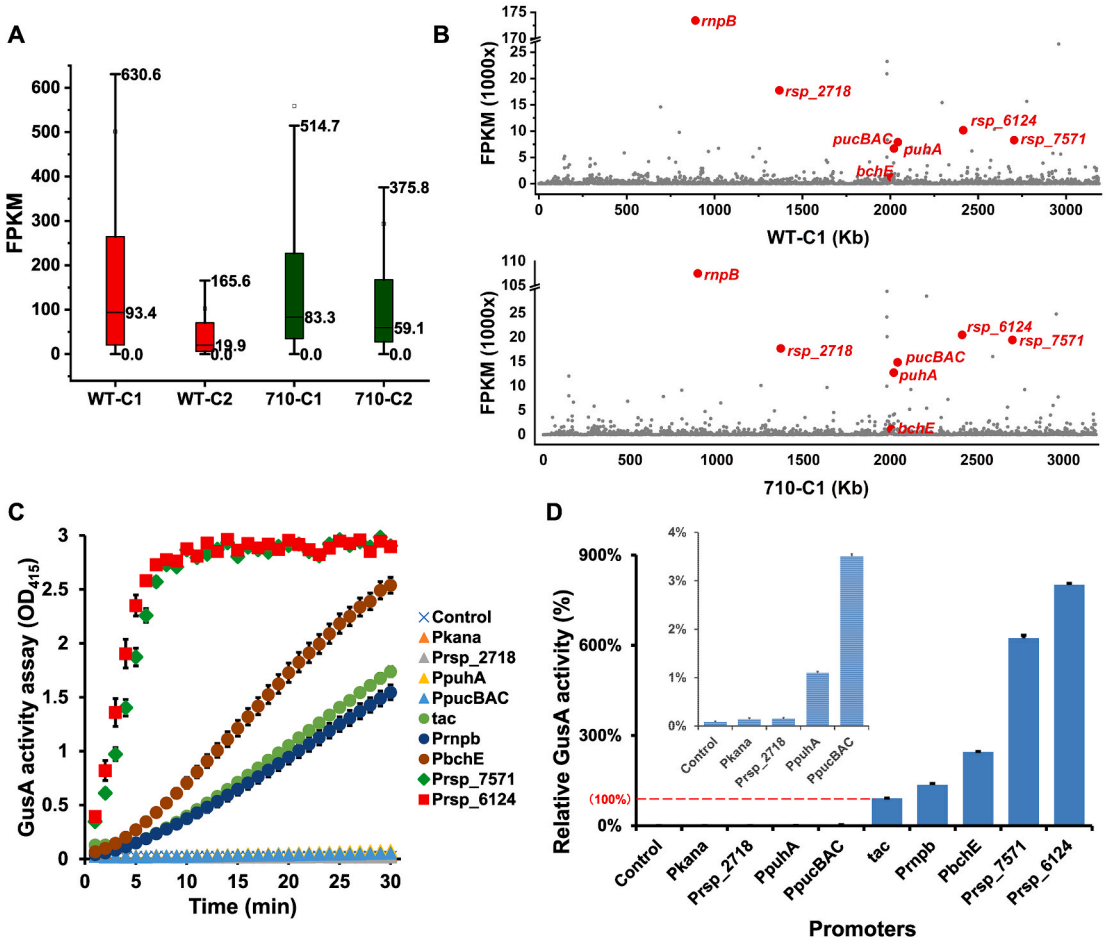

Fig. 1. Screening and characterization of selected candidate native promoters from *R. sphaeroides*. **A.** Box plot of the FPKM (Fragments Per Kilobase of transcript per Million fragments mapped) transcripts at 24 h for the two circular chromosomes in JDW-710 and WT. **B.** Transcription profile of chromosome I and the selected native promoters (highlighted in red) at 24 h in JDW-710 and WT. **C.** Evaluation of promoter strength by GusA enzymatic activity. **D.** Promoter strengths of the selected native and reference promoters in JDW-710. Control, JDW-710 containing the pBBR plasmid. Pkana, the kanamycin resistance gene promoter in the pBBR plasmid. The activity of *tac* was set to 100%. Data are expressed as the mean ± SEM. (For interpretation of the references to colour in this figure legend, the reader is referred to the Web version of this article.)

Both commercially available tryptic soy broth (TSB) medium and Q_{10} fermentation medium [13] were used. As shown in Fig. 2A and C, except for the decreased cell growth shown by P_{rsp_6124}, all other JDW-710 transformants containing different promoters exhibited no significant differences with respect to the control in both media. The activity of these promoters from the logarithmic phase to the stationary phase was also monitored, as shown in Fig. 2B, and the activity of P_{rsp_6124} and P_{rsp_7571} ranged from 600% to 836%, and 409%–640%, respectively, in TSB medium. In the Q_{10} fermentation medium, the activity of P_{rsp_6124} and P_{rsp_7571} ranged from 429% to 1234%, and 496%–888%, respectively (Fig. 2D). These results indicated that both P_{rsp_6124} and P_{rsp_7571} maintained high activity in different media and time periods. Although the activity of P_{rsp_6124} was stronger than that of P_{rsp_7571}, because of the former's inhibitory effects on cell growth, P_{rsp_7571} was selected for subsequent study.

3.3. Construction of the constitutive promoter library

The 500 bp upstream region of the open reading frame *rsp_7571* was arbitrarily selected as the original length P_{rsp_7571}, which probably contained some redundant sequences and was additionally too long for future applications. Therefore, before the creation of a library of synthetic promoters with different strengths, we attempted to shorten and simplify the sequence of P_{rsp_7571} by sequence truncation. As shown in Fig. 3A, three P_{rsp_7571}-derived promoters, T344, T167 and T84, were generated by truncation, and the spacing between the −10 and −35 consensus sequences in these P_{rsp_7571}-derived promoters was 18 bp. The activity of T84 was 90% lower than that of P_{rsp_7571} during the entire culture period (6–32 h), whereas the activity of T344 and T167 was approximately 50% lower (Fig. 3B). Although the sequence truncation decreased the promoter activity, T344 and T167 still had 3–4-fold higher activity than the *tac* promoter. Both T344 and T167 were used as error-prone PCR templates for subsequent promoter library construction (see Fig. 4).

Fig. 4A shows the entire workflow of the constitutive promoter library construction. Briefly, T334 and T167 were randomly mutated by error-prone PCR, and RFP was used for promoter screening. By using a portable fluorescence vision system, we were able to directly pick transformants with promoters with different activity from the agar plates according to fluorescence intensity. After the next step of inoculation and culture in 48-well microplates, the transformants were verified with a fluorescence reader. In this study, after further characterization, 20 of 67 synthetic promoters were selected (Fig. S2). The corresponding DNA sequence of each selected promoter is listed in Table S5. Most of the transformants (18/20) showed no significant differences in cell growth with respect to that of the control (transformant containing *tac* or P_{rsp_7571} promoters) (Fig. S3), and these synthetic promoters had strengths ranging from 54% to 2987% that of the *tac* promoter (Fig. 4B).

3.4. Upregulation of key biosynthetic genes for Q_{10} production

To demonstrate the application of these promoters, T334*, which showed similar activity to P_{rsp_7571}, was selected from the promoter library to upregulate the biosynthetic pathway for Q_{10} production in JDW-710. As shown in Fig. 5D, *dxs* and *ubiE* are two key genes involved in the methylerythritol phosphate (MEP) pathway and quinone modification, respectively [11,27]. In the subsequent fermentation, both *dxs* and *ubiE* were overexpressed under the control of T334* in JDW-710 (DOE2). Compared with that in the control (JDW:pBBR), the cell growth was slightly lower (10% in 48 h, and 7% in 72 h; Fig. 5A); however, the Q_{10} production increased by 18%, reaching 226 mg/L in 72 h ($P < 0.05$; Fig. 5B), and the Q_{10} yield increased 28% ($P < 0.05$; Fig. 5C). Furthermore, *dxs* and *ubiE* transcription in DOE2 was verified

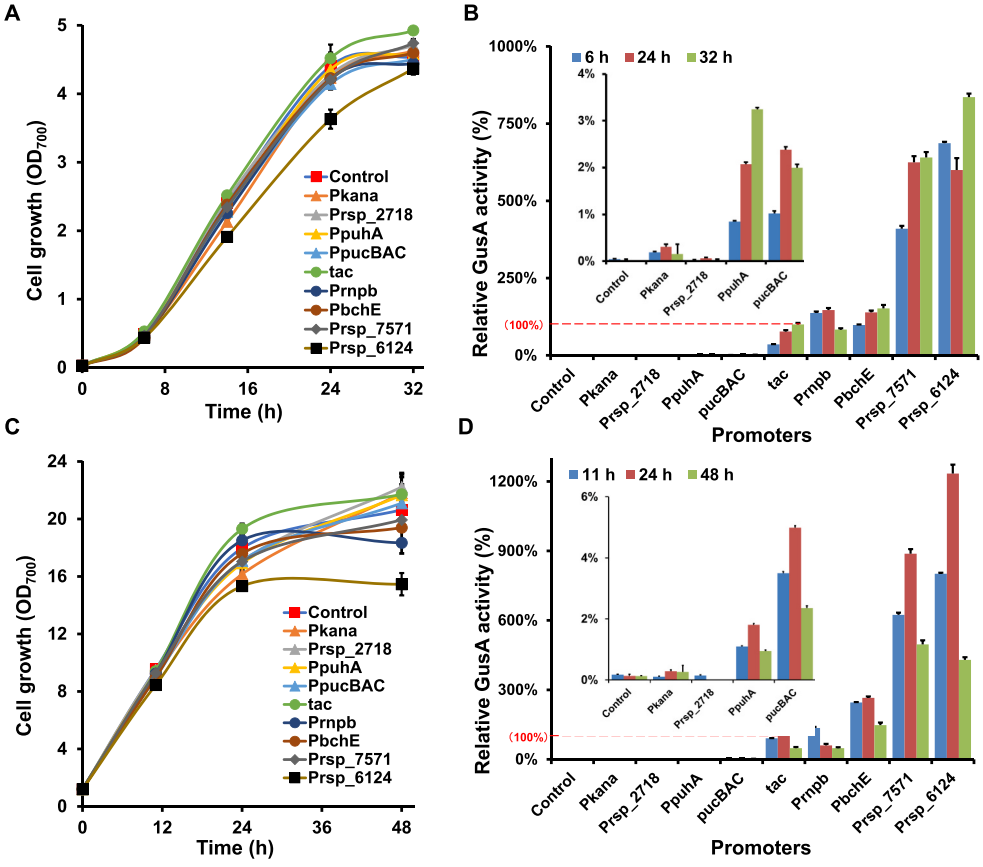

Fig. 2. Characterization of selected native promoters in different culture media and time periods. **A-B.** Cell growth and GusA activity of the JDW-710 transformants in TSB medium in shake flasks. Because of variations in tac activity, the maximum activity of *tac* (at 32 h) was set to an expression level of 100%. **C-D.** Cell growth and GusA activity of JDW-710 transformants in Q_{10} fermentation medium in shake flasks. JDW-710 containing the pBR322 plasmid served as the control. Because of the variation in tac activity, the maximum activity of tac (at 24 h) was set to an expression level of 100%. Control, JDW-710 containing the pBBR plasmid. Pkana, the kanamycin resistance gene promoter in the pBBR plasmid. Data are expressed as the mean ± SEM.

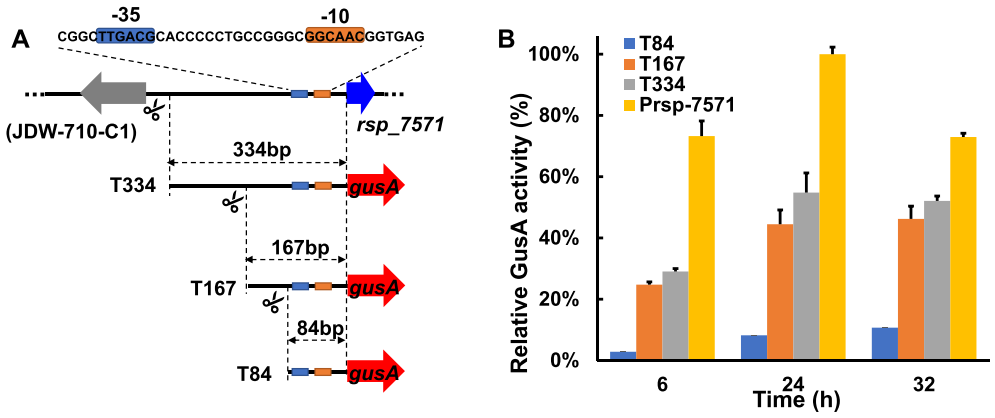

Fig. 3. Truncation and characterization of promoter P_{rsp_7571}. **A.** Truncation of the strong native promoter P_{rsp_7571}. T334 (334bp), T167 (167bp) and T84 (84bp) are three P_{rsp_7571}-derived promoters generated by sequence truncation. **B.** Relative GusA activity of truncated forms of P_{rsp_7571} in JDW-710 in TSB medium. The activity of P_{rsp_7571} at 24 h was set to an expression level of 100%.

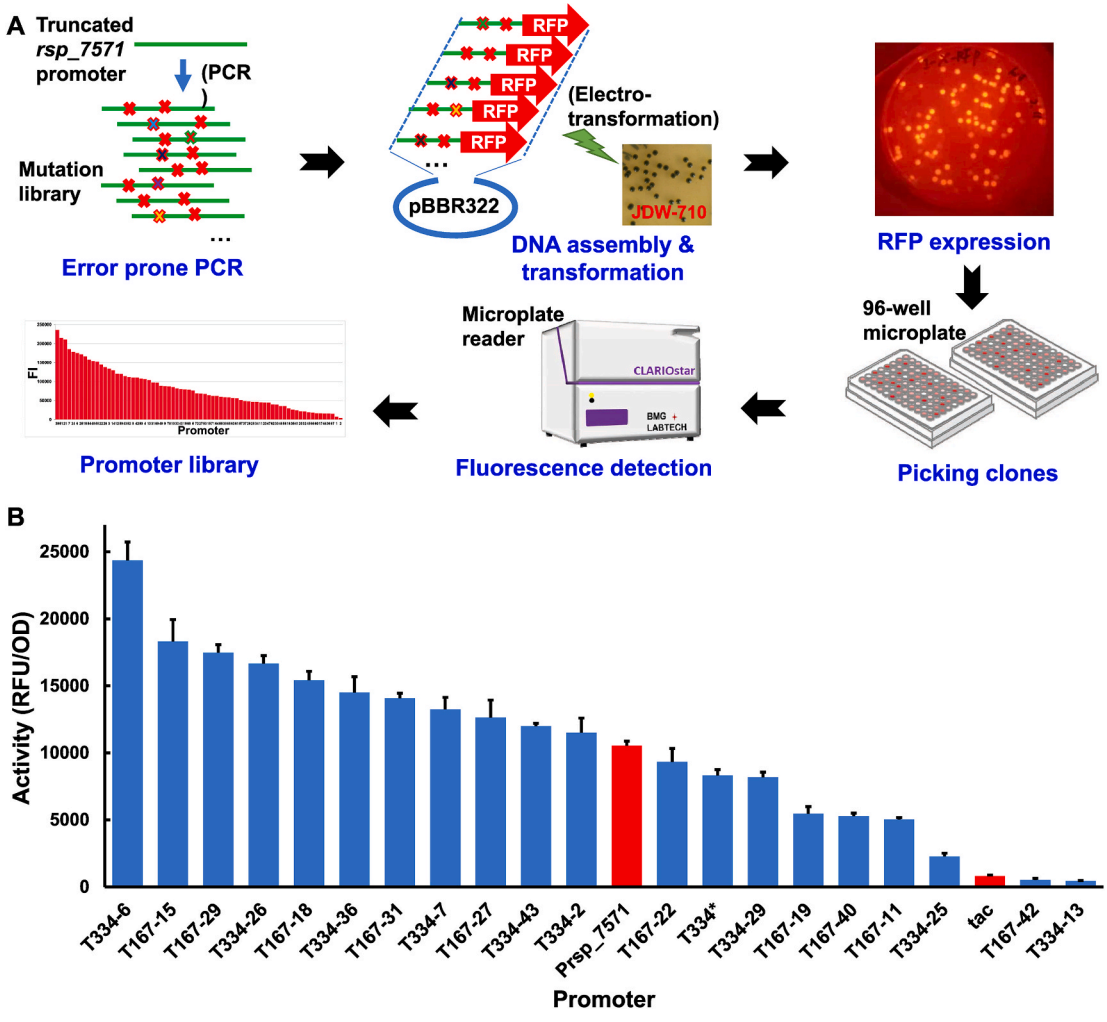

Fig. 4. Construction of the P_{rsp_7571}-derived promoter library. **A.** Workflow of constitutive promoter library construction using the visualized RFP reporter system. **B.** The strength of 21 sequenced synthetic promoters. P_{rsp_7571} and the *tac* promoter is highlighted in red. The activity (RFU, relative fluorescence units) of each promoter was calibrated by cell growth (OD_{700}). T334-xx and T167-xx represent T334-and T167-derived promoters, respectively. (For interpretation of the references to colour in this figure legend, the reader is referred to the Web version of this article.)

at 24 h, as shown in Fig. 5E–F, and the transcription of *dxs* and *ubiE* increased 38-fold and 27-fold, respectively ($P < 0.05$). Simultaneously, the *tac* promoter was used to overexpress *dxs* and *ubiE* in JDW-710. Although the transcription was greater than that in the control (JDW: pBBR), no significant effects on cell growth and Q_{10} production were observed (Fig. S4).

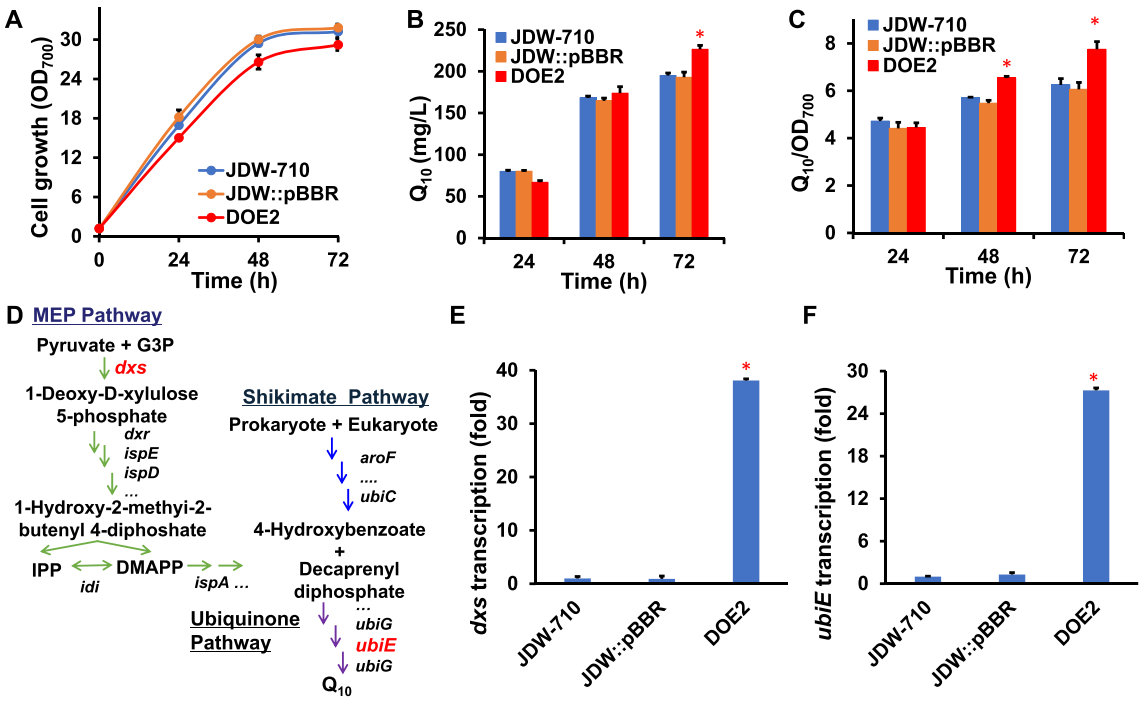

Fig. 5. Enhanced Q_{10} production achieved by engineering the synthetic pathway in JDW-710. **A-C.** Time course of cell growth, Q_{10} production and yield in shake-flask fermentation. **D.** Biosynthetic pathway of Q_{10} in *R. sphaeroides*. **E-F.** Transcriptional verification of *dxs* and *ubiE* expression in different strains in 24 h by q-PCR. The transcription of *dxs* and *ubiE* in JDW-710 (reference sample) was set to an expression level of 1.0, and the data for other strains are expressed as the fold increase of the mRNA level over the reference sample. JDW:pBBR (blank control), JDW-710 containing pBBR plasmid; DOE2 (JDW-710:pBBR-pT334*-dxs-ubiE), *dxs* and *ubiE* doubly overexpressed under the control of T334* in JDW-710; $*P < 0.05$.

4. Discussion

Construction and characterization of regulatory elements (*e.g.,* promoters and ribosomal binding sites) are strongly motivated by the need to precisely control the expression of target genes or pathways in different MCFs [23,25]. Despite being the widely used promoter in *R. sphaeroides*, the *tac* promoter has never been well characterized for its activity in this photosynthetic bacterium. On the basis of our previous experience [13], the strength of the *tac* promoter probably does not fully meet the requirements for gene overexpression. To resolve the lack of known regulatory elements in *R. sphaeroides*, this study focused on characterizing and engineering synthetic promoters.

Transcriptomic analysis-based screening of high activity native promoter candidates has been demonstrated previously [37]. To obtain a highly active native promoter with good universality in *R. sphaeroides*, we selected seven promoters showing good transcriptional consistency in different strains (JDW-710, WT) as candidates, on the basis of transcription profile analysis. However, the transcriptional activity and enzymatic activity were not always consistent and sometimes were opposite (*e.g.,* P_{rsp_2718}, P_{puhA}, P_{pucBAC}) (Fig. 1). A weak correlation between RNA and protein abundance has also been observed in a previous study [37], probably for a variety of reasons, such as post-transcriptional gene regulation (i.e., by small RNAs and RNA-binding proteins) and the activity of ribosomal binding sites [25,38]. Interestingly, the promoters of *rsp_6124* (97 amino acid residues) and *rsp_7571* (55 amino acid residues), both of which are annotated as hypothetical proteins, displayed a good correlation between RNA abundance (FPKM) and GusA enzymatic activity. Moreover, these two putative genes are highly sequence conserved in other photosynthetic bacteria beyond WT and JDW-710, such as *R. sphaeroides* KD131 (KCTC12085) [39], *R. sphaeroides* ATCC 17025 (AHT2.4.3) [40] and *R. sphaeroides* ATCC 17029 (AHT2.4.9) [40]. Although the biological function of these two hypothetical genes remains unknown, their broad distribution probably indicated the universality of these regulatory elements in different *R. sphaeroides*.

In subsequent *in vivo* characterization of the native promoters, during the entire fermentation period, both P_{rsp_6124} and P_{rsp_7571} showed high GusA enzymatic activity in both a glucose-rich fermentation medium [13] and a commercially available TSB medium. However, the application of P_{rsp_6124} significantly inhibited cell growth (Fig. 2). High copy numbers of the plasmids and high production of enzymes are known to hinder cell growth [41]. In this study, the activity of P_{rsp_6124} and P_{rsp_7571} was relatively similar, but the application of P_{rsp_7571} had no effects on cell growth. Moreover, after the truncation of P_{rsp_6124}, although the GusA enzymatic activity was ~40% lower than that of native P_{rsp_6124}, and the cell growth remained significantly inhibited (Fig. S5). Therefore, the inhibitory effects of P_{rsp_6124} on cell growth were probably due to some unknown mechanism, a possibility requiring further investigation.

Although detection of the enzymatic activity of GusA in protein extracts is a sensitive and versatile method, that has been used in promoter library screening [23,42], it remains a cumbersome, labor-intensive process. In addition, on the basis of our preliminary results (data not shown), we found that in the *R. sphaeroides* culture system, the red fluorescence had a relatively high sensitivity, low background and no interference from the medium or intracellular metabolites, *e.g.*, bacteriochlorophyll and carotenoids [43]. Consequently, we used a portable red fluorescence visualization system to directly screen the promoters with different strengths on the basis of fluorescence intensity (Fig. 4). With this RFP visualization system, the promoter library was rapidly and efficiently constructed. After several rounds of mutation and screening, each well-characterized promoter sequence in the library had three to seven site mutations, as compared with the native promoter sequence. This panel of P_{rsp_7571}-derived synthetic promoters with higher sequence diversity may have merit in applications [44].

T344 and T167, two P_{rsp_7571}-derived promoters created by sequence truncation (Fig. 3), contain both the promoter region and the native ribosomal binding site (RBS) region. During the error-prone PCR amplification in library construction, mutagenesis of only the promoter region was performed. The resulting well-characterized synthetic

constitutive promoters had strengths ranging from 54% (T334-13) to 2987% (T334-6) that of the *tac* promoter. Furthermore, that RBSs are important biobricks for controlling the expression of target genes [45]. Through use of the RFP visualization system and the current synthetic promoters combined with the RBS library with different ribosome binding affinities, more diversified regulatory elements could be generated [25].

As a high value-added nutraceutical, Q_{10} is widely used to prevent cardiovascular disease [46]. However, to date, no metabolic engineering strategies have achieved Q_{10} overproduction in a high-producing industrial strain [13]. To demonstrate the application of these synthetic promoters in synthetic pathway refactoring, we used the selected promoter T334*, which showed similar activity to P_{rsp_7571}, to strengthen the Q_{10} synthetic pathway in JDW-710. In Q_{10} production, *dxs* and *ubiE* are two known bottleneck genes [11,27]. However, use of the *tac* promoter does not significantly affect Q_{10} production in JDW-710. Owing to the higher activity of T334* (920% higher than that of *tac*) and moderate copy number of pBBR plasmid (~10 copies per cell) [47], the transcription of *dxs* and *ubiE* increased 38-fold and 27-fold, respectively, under the same strategy. The Q_{10} yield increased 28%, and Q_{10} production reached 226 mg/L in DOE2 (Fig. 5). Although the Q_{10} production in DOE2 must be further improved beyond that in a previous study [13], these results indicated that a highly active promoter element was a requirement for successful engineering of a high-producing industrial strain. Beyond the slight inhibition of cell growth by using T334*, we found that the concentration of bacteriochlorophyll significantly increased in DOE2 (Fig. S6), indicating that the terpenoid precursor (*e.g.,* geranylgeranyl pyrophosphate) supply for the downstream pathway was also upregulated [48]. Future fine tuning of promoter activity and the metabolic flux toward Q_{10} biosynthesis is needed to improve the yield of the Q_{10} high-producing industrial strain.

5. Conclusion

In summary, on the basis of transcriptomics analysis of two types of *R. sphaeroides* and enzymatic activity verification, we identified P_{rsp_7571} as a native highly active promoter. Through random sequence mutation and the use of an RFP visualization screening system, we constructed a P_{rsp_7571}-derived synthetic promoter library. Finally, a selected strong synthetic promoter was used to significantly improved the Q_{10} biosynthetic efficiency in a high-producing industrial strain. These well-characterized promoters should be highly useful in current synthetic biology platforms for refactoring the biosynthetic pathway in *R. sphaeroides*-derived MCFs.

5.1. Associated content

The Supporting Information is available free of charge online. Tables S1–S5; Figs. S1–S6.

The authors declare that they have no conflicts of interest to disclose. All authors read the manuscript and agreed to submit to Biosensors and Bioelectronics.

Tong, Tong Shi: Investigation, Methodology, Visualization, Formal analysis. Lu Zhang: Investigation, Methodology, Visualization, Formal analysis. Mindong Liang: Investigation, Methodology, Visualization, Formal analysis. Weishan Wang: Investigation, Methodology, Visualization. Kefeng Wang: Investigation, Methodology, Visualization. Yue Jiang: Investigation, Methodology, Visualization. Jing Liu: Investigation, Methodology, Visualization. Xinwei He: Investigation, Methodology. Zhiheng Yang: Methodology. Haihong Chen: Methodology. Chuan Li: Methodology. Dongyuan Lv: Methodology. Liming Zhou: Methodology. Biqin Chen: Resources. Dan Li: Resources. Li-Xin Zhang: Supervision, Funding acquisition. Gao-Yi Tan: Supervision, Funding acquisition, Conceptualization, Writing - Original Draft, Writing - Review & Editing.

Acknowledgments

This work was supported by the National Natural Science Foundation of China [31870040], the National Key Research and Development Project (2020YFA0907804, 2020YFA0907304), the "111" Project of China [B18022], the Fundamental Research Funds for the Central Universities [22221818014], and the Open Project Funding of the State Key Laboratory of Bioreactor Engineering.

Appendix A. Supplementary data

Supplementary data to this article can be found online at https://doi.org/10.1016/j.synbio.2021.09.011.

References

[1] Paddon CJ, Westfall PJ, Pitera DJ, Benjamin K, Fisher K, McPhee D, Leavell MD, Tai A, Main A, Eng D, et al. High-level semi-synthetic production of the potent antimalarial artemisinin. Nature 2013;496(7446):528–32.
[2] Galanie S, Thodey K, Trenchard IJ, Filsinger Interrante M, Smolke CD. Complete biosynthesis of opioids in yeast. Science 2015;349(6252):1095.
[3] Tan G-Y, Zhu F, Deng Z, Liu T. In vitro reconstitution guide for targeted synthetic metabolism of chemicals, nutraceuticals and drug precursors. Synth Syst Biotechnol 2016;1(1):25–33.
[4] Tan G-Y, Liu T. Rational synthetic pathway refactoring of natural products biosynthesis in actinobacteria. Metab Eng 2017;39:228–36.
[5] Li S, Yang B, Tan G-Y, Ouyang L-M, Qiu S, Wang W, Xiang W, Zhang L. Polyketide pesticides from actinomycetes. Curr Opin Biotechnol 2021;69:299–307.
[6] Yang Z, Sun Q, Tan G, Zhang Q, Wang Z, Li C, Qi F, Wang W, Zhang L, Li Z. Engineering thermophilic *Geobacillus thermoglucosidasius* for riboflavin production. Microb Biotechnol 2021;14(2):363–73.
[7] Chen G-Q, Jiang X-R. Next generation industrial biotechnology based on extremophilic bacteria. Curr Opin Biotechnol 2018;50:94–100.
[8] Jungas C, Ranck J-L, Rigaud J-L, Joliot P, Vermeglio A. Supramolecular organization of the photosynthetic apparatus of *Rhodobacter sphaeroides*. EMBO J 1999;18(3):534–42.
[9] Orsi E, Beekwilder J, Eggink G, Kengen SWM, Weusthuis RA. The transition of Rhodobacter sphaeroides into a microbial cell factory. Biotechnol Bioeng 2020;18(2):531–41.
[10] Lee SQE, Tan TS, Kawamukai M, Chen ES. Cellular factories for coenzyme Q_{10} production. Microb Cell Factories 2017;16(1):39.
[11] Lu W, Ye L, Lv X, Xie W, Gu J, Chen Z, Zhu Y, Li A, Yu H. Identification and elimination of metabolic bottlenecks in the quinone modification pathway for enhanced coenzyme Q_{10} production in Rhodobacter sphaeroides. Metab Eng 2015;29:208–16.
[12] Wang Z-J, Zhang X, Wang P, Sui Z, Guo M, Zhang S, Zhuang Y. Oxygen uptake rate controlling strategy balanced with oxygen supply for improving coenzyme Q_{10} production by *Rhodobacter sphaeroides*. Biotechnol Bioproc Eng 2020;25(3):459–69.
[13] Zhang L, Liu L, Wang K-F, Xu L, Zhou L, Wang W, Li C, Xu Z, Shi T, Chen H, et al. Phosphate limitation increases coenzyme Q_{10} production in industrial *Rhodobacter sphaeroides* HY01. Synth Syst Biotechnol 2019;4(4):212–9.
[14] Su A, Chi S, Li Y, Tan S, Qiang S, Chen Z, Meng Y. Metabolic redesign of *Rhodobacter sphaeroides* for lycopene production. J Agric Food Chem 2018;66(23):5879–85.
[15] Qiang S, Su AP, Li Y, Chen Z, Hu CY, Meng YH. Elevated β-carotene synthesis by the engineered *Rhodobacter sphaeroides* with enhanced CrtY expression. J Agric Food Chem 2019;67(34):9560–8.
[16] Orsi E, Mougiakos I, Post W, Beekwilder J, Dompè M, Eggink G, van der Oost J, Kengen SWM, Weusthuis RA. Growth-uncoupled isoprenoid synthesis in Rhodobacter sphaeroides. Biotechnol Biofuels 2020;13(1):123.
[17] Qu Y, Su A, Li Y, Meng Y, Chen Z. Manipulation of the regulatory genes ppsR and prrA in Rhodobacter sphaeroides enhances lycopene production. J Agric Food Chem 2021;69(14):4134–43.
[18] Kang Z, Zhang J, Zhou J, Qi Q, Du G, Chen J. Recent advances in microbial production of δ-aminolevulinic acid and vitamin B_{12}. Biotechnol Adv 2012;30(6):1533–42.
[19] Hu J, Yang H, Wang X, Cao W, Guo L. Strong pH dependence of hydrogen production from glucose by *Rhodobacter sphaeroides*. Int J Hydrogen Energy 2020;45(16):9451–8.
[20] Li S, Sakuntala M, Song YE, Heo J-o, Kim M, Lee SY, Kim M-S, Oh Y-K, Kim JR. Photoautotrophic hydrogen production of *Rhodobacter sphaeroides* in a microbial electrosynthesis cell. Bioresour Technol 2021;320:124333.
[21] Mougiakos I, Orsi E, Ghiffary MR, Post W, de Maria A, Adiego-Perez B, Kengen SWM, Weusthuis RA, van der Oost J. Efficient Cas9-based genome editing of *Rhodobacter sphaeroides* for metabolic engineering. Microb Cell Factories 2019;18(1):204.
[22] Luo Y, Ge M, Wang B, Sun C, Wang J, Dong Y, Xi JJ. CRISPR/Cas9-deaminase enables robust base editing in *Rhodobacter sphaeroides* 2.4.1. Microb Cell Factories 2020;19(1):93.

[23] Siegl T, Tokovenko B, Myronovskyi M, Luzhetskyy A. Design, construction and characterisation of a synthetic promoter library for fine-tuned gene expression in actinomycetes. Metab Eng 2013;19:98–106.
[24] Wang W, Li X, Wang J, Xiang S, Feng X, Yang K. An engineered strong promoter for streptomycetes. Appl Environ Microbiol 2013;79(14):4484–92.
[25] Bai C, Zhang Y, Zhao X, Hu Y, Xiang S, Miao J, Lou C, Zhang L. Exploiting a precise design of universal synthetic modular regulatory elements to unlock the microbial natural products in *Streptomyces*. Proc Natl Acad Sci U S A 2015;112(39):12181–6.
[26] Lu W, Shi Y, He S, Fei Y, Yu K, Yu H. Enhanced production of CoQ_{10} by constitutive overexpression of 3-demethyl ubiquinone-9 3-methyltransferase under tac promoter in *Rhodobacter sphaeroides*. Biochem Eng J 2013;72:42–7.
[27] Lu W, Ye L, Xu H, Xie W, Gu J, Yu H. Enhanced production of coenzyme Q_{10} by self-regulating the engineered MEP pathway in *Rhodobacter sphaeroides*. Biotechnol Bioeng 2014;111(4):761–9.
[28] Xu M, Wu H, Shen P, Jiang X, Chen X, Lin J, Huang J, Qi F. Enhancement of NADPH availability for coproduction of coenzyme Q_{10} and farnesol from *Rhodobacter sphaeroides*. J Ind Microbiol Biotechnol 2020;47(2):263–74.
[29] Wu X, Ma G, Liu C, Qiu X-y, Min L, Kuang J, Zhu L. Biosynthesis of pinene in purple non-sulfur photosynthetic bacteria. Microb Cell Factories 2021;20(1):101.
[30] Ind AC, Porter SL, Brown MT, Byles ED, de Beyer JA, Godfrey SA, Armitage JP. Inducible-expression plasmid for *Rhodobacter sphaeroides* and *Paracoccus denitrificans*. Appl Environ Microbiol 2009;75(20):6613.
[31] Lee JK, Kaplan S. cis-acting regulatory elements involved in oxygen and light control of puc operon transcription in Rhodobacter sphaeroides. J Bacteriol 1992;174(4):1146–57.
[32] Kobayashi J, Kondo A. Disruption of poly (3-hydroxyalkanoate) depolymerase gene and overexpression of three poly (3-hydroxybutyrate) biosynthetic genes improve poly (3-hydroxybutyrate) production from nitrogen rich medium by Rhodobacter sphaeroides. Microb Cell Factories 2019;18(1):40.
[33] Tan G-Y, Peng Y, Lu C, Bai L, Zhong J-J. Engineering validamycin production by tandem deletion of γ-butyrolactone receptor genes in *Streptomyces hygroscopicus* 5008. Metab Eng 2015;28:74–81.
[34] Tan G-Y, Bai L, Zhong J-J. Exogenous 1,4-butyrolactone stimulates A-factor-like cascade and validamycin biosynthesis in *Streptomyces hygroscopicus* 5008. Biotechnol Bioeng 2013;110(11):2984–93.
[35] Livak KJ, Schmittgen TD. Analysis of relative gene expression data using real-time quantitative PCR and the $2^{-\Delta\Delta CT}$ method. Methods 2001;25(4):402–8.
[36] Suwanto A, Kaplan S. Physical and genetic mapping of the *Rhodobacter sphaeroides* 2.4.1 genome: presence of two unique circular chromosomes. J Bacteriol 1989;171(11):5850.
[37] Luo Y, Zhang L, Barton KW, Zhao H. Systematic identification of a panel of strong constitutive promoters from *Streptomyces albus*. ACS Synth Biol 2015;4(9):1001–10.
[38] Van Assche E, Van Puyvelde S, Vanderleyden J, Steenackers HP. RNA-binding proteins involved in post-transcriptional regulation in bacteria. Front Microbiol 2015;6:141.
[39] Lim S-K, Kim SJ, Cha SH, Oh Y-K, Rhee H-J, Kim M-S, Lee JK. Complete genome sequence of *Rhodobacter sphaeroides* KD131. J Bacteriol 2009;191(3):1118–9.
[40] Choudhary M, Zanhua X, Fu YX, Kaplan S. Genome analyses of three strains of *Rhodobacter sphaeroides*: evidence of rapid evolution of chromosome II. J Bacteriol 2007;189(5):1914–21.
[41] Malakar P, Venkatesh KV. Effect of substrate and IPTG concentrations on the burden to growth of *Escherichia coli* on glycerol due to the expression of Lac proteins. Appl Microbiol Biotechnol 2012;93(6):2543–9.
[42] Myronovskyi M, Welle E, Fedorenko V, Luzhetskyy A. Beta-glucuronidase as a sensitive and versatile reporter in actinomycetes. Appl Environ Microbiol 2011;77(15):5370–83.
[43] Penfold RJ, Pemberton JM. Sequencing, chromosomal inactivation, and functional expression in *Escherichia coli* of ppsR, a gene which represses carotenoid and bacteriochlorophyll synthesis in *Rhodobacter sphaeroides*. J Bacteriol 1994;176(10):2869–76.
[44] Wang B, Kitney RI, Joly N, Buck M. Engineering modular and orthogonal genetic logic gates for robust digital-like synthetic biology. Nat Commun 2011;2(1):508.
[45] Dong H, Zhao C, Zhang T, Zhu H, Lin Z, Tao W, Zhang Y, Li Y. A systematically chromosomally engineered *Escherichia coli* efficiently produces butanol. Metab Eng 2017;44:284–92.
[46] Ayer A, Macdonald P, Stocker R. CoQ_{10} function and role in heart failure and ischemic heart disease. Annu Rev Nutr 2015;35(1):175–213.
[47] Elzer PH, Kovach ME, Phillips RW, Robertson GT, Peterson KM, Roop RM. In vivo and in vitro stability of the broad-host-range cloning vector pBBR1MCS in six brucella species. Plasmid 1995;33(1):51–7.
[48] Chen GE, Canniffe DP, Barnett SFH, Hollingshead S, Brindley AA, Vasilev C, Bryant DA, Hunter CN. Complete enzyme set for chlorophyll biosynthesis in *Escherichia coli*. Sci Adv 2018;4(1):eaaq1407.